Published in final edited form as:
Int J Radiat Oncol Biol Phys. 2010 July 1; 77(3): 910–917. doi:10.1016/j.ijrobp.2009.09.080.

Anatomical and Pathological Variability during Radiation Therapy for a Hybrid Active Breath Hold Gating Technique

Carri K. Glide-Hurst, Ph.D.[a], **Ellen Gopan, M.S.**[a,b], and **Geoffrey D. Hugo, Ph.D.**[c]

[a] Department of Radiation Oncology William Beaumont Hospital Royal Oak, Michigan U.S.A.

[b] Wayne State University Detroit, Michigan U.S.A.

[c] Department of Radiation Oncology Virginia Commonwealth University Richmond, Virginia U.S.A.

Abstract

Purpose—To evaluate intra- and inter-fraction variability of tumor and lung volume and position using a hybrid active breath-hold gating technique.

Methods and Materials—159 repeat normal inspiration active breath-hold CTs were acquired weekly during radiation therapy for 9 lung cancer patients (12-21 scans/patient). A physician delineated the gross tumor volume (GTV), lungs, and spinal cord on the first breath-hold CT and contours were propagated semi-automatically. Intra- and inter-fraction variability of tumor and lung position and volume were evaluated. Tumor centroid and border variability was quantified.

Results—On average, intra-fraction variability of lung and GTV centroid position was less than 2.0 mm. Inter-fraction population variability was 3.6-6.7 mm (systematic) and 3.1-3.9 mm (random) for the GTV centroid and 1.0-3.3 mm (systematic) and 1.5-2.6 mm (random) for the lungs. Tumor volume regressed 44.6% ± 23.2%. GTV border variability was patient-specific and demonstrated non-isotropic shape change in some subjects. Inter-fraction GTV positional variability was associated with tumor volume regression and contralateral lung volume ($p < 0.05$). Inter-breath hold reproducibility was unaffected by time point in the treatment course ($p > 0.1$). Increases in free-breathing tidal volume were associated with increases in breath-hold ipsilateral lung volume ($p < 0.05$).

Conclusions—The breath hold technique was reproducible within 2 mm during each fraction. Inter-fraction variability of GTV position and shape was substantial due to tumor volume and breath hold lung volume change during therapy. These results support the feasibility of a hybrid breath-hold gating technique and suggest online image guidance would be beneficial.

Keywords

Active breath-hold; Respiratory motion; Lung cancer; Intra-fraction variability, Inter-fraction variability

Corresponding Author: Geoffrey D. Hugo, Ph.D. Virginia Commonwealth University 401 College St., P.O. Box 980058. Richmond, VA 23298 Phone: 804-628-3457 Fax: 804-628-0271 gdhugo@vcu.edu.

Conflict of interest: William Beaumont Hospital holds a research agreement with Elekta Oncology Systems.

INTRODUCTION

One impediment in the precise delivery of thoracic radiotherapy is the effect of respiratory-induced tumor motion. Considerable effort has been made to characterize lung tumor motion due to respiration and its variation during treatment (1-7). The results of these studies support the overall recommendation of assessing tumor motion on a patient-specific basis, and motion management approaches have been recommended for tumor excursion greater than 5 mm in any direction (8).

Active breathing control, or ABC, has proven to be effective in stabilizing both the lung volume and lung tumor position (9-14). This supports the implementation of ABC for lung cancer radiotherapy, however lung tumor stability and breath-hold reproducibility late in the treatment course has not been widely explored. A study conducted by Kashani *et al.* explored lung tumor short and long-term stability under moderate deep inspiration (i.e. 75-80% of vital capacity), half the volume of inhale, and end exhale breath-hold at three different time points during treatment (12). This study was limited to evaluating reproducibility of the target volume position as represented by the centroid. Long-term breath-hold stability is of particular importance in lung cancer radiotherapy due to initial compromised pulmonary function that may be exacerbated by radiation and chemotherapy regimens, as previously reported for breast cancer patients (15,16).

Furthermore, evaluating tumor stability over time is of interest due to changes in the respiratory pattern (2) and tumor motion that have been observed throughout radiation therapy. Britton *et al*. analyzed repeat 4DCTs and demonstrated that tumor mobility changes significantly throughout treatment (1). Similarly, Nottrup et al. evaluated breathing variation for eleven patients via external monitoring with the Varian RPM system and reported a median population variation of ~15 mm (intra- and inter-fraction variations combined) over the treatment course, with baseline variation being the largest individual component (3). Because the ABC device is not an absolute spirometer—baseline levels are set to the functional residual capacity (end of normal expiration) throughout the breathing session (13)— changes in breathing pattern over the treatment course may lead to changes in the predefined volume of breath-hold. In addition, the effects of tumor volume regression and other pathological changes over time, which have been shown to contribute to changes in lung tumor position in free-breathing radiotherapy (17), cannot be overlooked. All of these studies provide compelling evidence that evaluating patient performance and lung tumor stability with ABC over the treatment course is necessary.

One issue impeding the widespread implementation of ABC for lung cancer radiotherapy is patient compliance. This is particularly true in the case of deep-inspiration breath-hold, where a reported 60% of lung cancer patients studied at one institution cannot perform breath-holds reproducibly enough to be treated with the device (8). Therefore, in an effort to improve patient compliance and tolerance to ABC, we designed a hybrid breath-hold gating technique at our institution. Similar to Murphy *et al.* (18), breath-hold levels were designed to follow normal patient respiration. For treatment, patients will be allowed to perform short (5 to 15 s) breath holds to reduce fatigue. The purpose of this study was to evaluate the intra- and inter-fraction stability of the lung tumor and lungs obtained throughout the radiation therapy treatment course using this hybrid breath-hold gating technique. Through this analysis, the feasibility of implementing ABC in lung cancer radiotherapy can be assessed, particularly late in the treatment course, where patient performance and breathing stability may be affected.

METHODS AND MATERIALS

Patient population

Nine patients with biopsy-confirmed non-small cell lung carcinoma were enrolled in an imaging study approved by William Beaumont Hospital's institutional review board after providing informed consent. Tumor location, pathology, and size varied, as demonstrated by Table 1. The mean patient age was 72.8 ± 11.5 years (range, 51-84). All but one patient (Patient 2) received concurrent chemotherapy with radiotherapy with the following regimens: carboplatin-taxol (n = 4) and cisplatin-etoposide (n = 4).

Active Breathing Coordinator

The Active Breathing Coordinator (Elekta, version 2.0) was used to maintain patient breath-hold. Subjects were initially coached to set individual levels of normal inspiration breath-hold for each patient and to familiarize them with the device. Breath-hold levels were set to approximately 80% of the normal tidal volume on inhalation (mean threshold volume = 0.84 ± 0.4 L). Breath-hold length was ~10-12 seconds, determined by the length of time required for helical CT scan acquisition.

CT image acquisition

CT acquisitions were performed on a multi-slice helical CT simulator (Brilliance Big Bore; Philips Medical Systems, Andover, MA). Once per week, either before or after radiation treatment, each patient received three successive CT scans while immobilized in the treatment position. Images were acquired under normal inspiration active breath hold at the threshold level determined in the initial coaching session. Patients were not repositioned between the three scans to enable an assessment of inter-breath hold reproducibility. All images were acquired with: 3 mm slice thickness and reconstructed with 2 mm slice thickness, pitch of 1.063, rotation time of 0.5 seconds, and collimator size of 16 × 1.5 cm. Over 4-7 imaging sessions, 12-21 helical CT scans were acquired per patient for a total of 159 breath-hold scans.

Contour delineation

All contours were delineated on the first ABC CT scan acquired. Using the clinical planning CT and PET-CT registered to the bony anatomy for guidance, the gross tumor volumes (GTV) were delineated by a physician. Only the primary tumors were delineated and analyzed as intravenous contrast was not used on a weekly basis to assist with nodal delineation. In addition, the right lung, left lung, and spinal cord were defined on the initial CT scan. For delineating the lungs and spinal cord, consideration was give nto ensure the organs spanned slices common to all weekly scan volumes. This prevented volumes from being drawn outside of the reconstructed volume on any scan. Contours were propagated to all other ABC-CTs using deformable image registration and automatic contour propagation as described in the next section.

Deformable Image Registration

All images were rigidly registered to the reference image (i.e. ABC session 1, CT scan 1) to align bony anatomy manually (Syntegra module of Pinnacle, Philips Medical Systems, Milpitas, CA). Intensity-based deformable image registration and semi-automatic contour propagation were implemented using in-house software previously described (19). This process generated displacement vectors for each image voxel that represented the 3D displacement between the reference and subsequent scan. A physician delineated the target and critical structures on the reference image, binary contour masks were created, and contours for the remaining ABC CTs were propagated using the displacement vectors. Contours were

visually inspected by a physician for agreement with their corresponding image sets and adjusted as needed.

Intra- and Inter-fraction Analysis

For each patient, inter-breath hold reproducibility was calculated for each session and for the total course. For each session, the standard deviation of the tumor centroid was calculated over the three successive scans from the session. The root mean square over all sessions for a patient was calculated to provide the mean inter-breath hold reproducibility over the treatment course. The inter-breath hold reproducibility of the lung and spinal cord centroids were calculated similarly. Variation in inter-breath hold reproducibility from the start of the treatment course to the end was evaluated using an *F*-test. The daily mean position for each session was calculated as the mean position of the structure centroid over the three successive scans. To assess the per-patient systematic and random variability, the mean and standard deviation of this daily position over all sessions was calculated. The overall systematic (Σ) and random (σ) variability were computed for the study population to enable margin calculation.

Due to response-induced shape changes, GTV centroid may not represent the overall positional variation of the GTV. We evaluated the positional variation of the GTV borders. A bounding box was constructed surrounding the GTV on each image. The coordinates of the corners with the minimum and maximum positions were recorded (the minimum corner corresponded to the right, posterior, superior corner of the GTV and the maximum corner was the left, anterior, inferior corner). Following the described method for the GTV centroid, the mean and standard deviation of the bounding box corner positions were calculated for each patient and the population as a measure of inter-fraction variability of the GTV borders.

The maximum variability may not necessarily be aligned along one of the cardinal (L-R, A-P, S-I) axes. To quantify the magnitude of maximum interfraction random variability for each patient, a method similar to that described by Lotz et al. (20) was used. For each patient, principal components analysis of the 3D coordinates of the GTV centroid daily position was performed. The resulting first principal component was selected for each patient, and the standard deviation of the centroid position projected along the first principal component axis was calculated. This process was repeated for the minimum and maximum bounding box corner positions.

The daily GTV position may be influenced by changes in the GTV volume due to tumor response, pathological (distal collapse, atelectasis, pleural effusion, etc.) changes which change the lung volume, or differences in daily lung volume at breath hold. To determine the magnitude of these effects, univariate and multivariate analyses were conducted with GTV daily position as the dependent variable, and the GTV, ipsi- and contra-lateral lung volumes each as independent variables.

Changes in breathing pattern throughout radiotherapy may lead to changes in the breath hold lung volume. To assess this effect for the patient population, the tidal volume as measured with the ABC device during free-breathing between breath holds over all breathing sessions was tabulated. The change in mean daily tidal volume (during free-breathing only) was calculated for each patient for each session, in relation to that patient's first session mean daily tidal volume. The mean change (M_μ) and standard deviation (Σ_μ) of change in daily tidal volume was calculated for the study population. To indicate changes in breathing pattern shape, the mean (M_μ) and standard deviation (Σ_σ) were calculated based on the change in standard deviation of the daily tidal volume. The impact of tumor regression and time point in the treatment course on tidal volume was evaluated.

Margin Evaluation

A population margin (M) for the GTV centroid was generated using the following two-parameter population margin equation introduced in van Herk *et al.* (21):

$$M=2.5\Sigma+1.64\sqrt{\sigma^2+\sigma_p^2}-1.64\sigma_p \quad (1)$$

Here, Σ and σ are the standard deviation of the systematic and root mean square random error of GTV centroid for the patient population, respectively, while σ_p describes the width of penumbra in lung as modeled by a Gaussian (taken to be 6.4 mm as described in Sonke *et al.* (7)).

RESULTS

Intra-fraction Variability

Table 2 demonstrates the inter–breath hold GTV and lung reproducibility for the patient population over all imaging sessions. On average, the lung centroid positions had an inter-breath hold variability of 0.52, 0.98, and 1.98 mm in L-R, A-P, and S-I directions, respectively. Inter-breath hold (intrafraction) reproducibility of the GTV position was unaffected by time point in the treatment course in all directions, (*F* test, $p > 0.1$). For the spinal cord (results not shown), which is not expected to be affected by breath-hold, the inter-breath hold variability of the centroid was found to be 0.2 ± 0.2, 0.3 ± 0.2, and 1.0 ± 0.5 mm in L-R, A-P, and S-I directions, respectively.

Inter-fraction Variability

The inter-fraction variability in GTV centroid position (all directions) ranged from 3.6 (LR) to 6.7 (SI) mm for the systematic component and 3.1 to 3.9 mm for the random component (Table 3). The inter-fraction variability was most substantial in the superior to inferior direction. The population margin required to compensate for all variability in the GTV centroid for this population would be 8.6 mm, 9.4 mm, and 16.4 mm in the LR, AP, and SI directions, respectively.

Table 4 shows the GTV border variability determined by bounding box analysis for the study population. The group means for the left and posterior borders are large due to Patients 4 and 7 having greater than 10 mm systematic errors for these borders. Generally, the border variation in the S-I direction was largest, although the border exhibiting maximum variability was highly patient-dependent. Table 5 shows the maximum variability of the bounding box corners and centroid oriented along the arbitrary axis of maximum variability. The largest variability in the group and the largest difference in variability between the bounding box corners was observed for Patients 4 and 7. These subjects also exhibited the most tumor volume regression during treatment.

Three patients (4, 6, and 7) had individual systematic displacements in GTV centroid greater than 5.0 mm relative to bone. Patient 4 exhibited a 13.5 mm centroid systematic error in the SI direction, with the daily tumor centroid becoming more superior as treatment progressed. The inferior tumor border systematic error was 16.0 mm, while the superior border systematic error was 4.2 mm. For this patient, non-uniform regression of the tumor volume manifested as a trend in tumor centroid during treatment (Figure 1). For all patients, tumor volume regressed an average of 44.6% (range: 16.7-81.3%) over the treatment course, with Figure 2 demonstrating weekly changes in GTV volume for all 9 patients. Both systematic and random inter-fraction GTV centroid variability were strongly associated with total tumor reduction over the treatment course ($r^2 = 0.74$ and 0.58, respectively). The minimum and maximum

bounding box positions were also associated (r^2 = 0.51 and 0.61, respectively) with tumor reduction as well.

For both lungs combined, the inter-fraction variability of the daily centroid position ranged from 1.0 to 3.3 mm and 1.5 to 2.6 mm for systematic and random components, respectively. Figure 3 shows the average left lung volume throughout the treatment course for each patient. Similar results were obtained for the right lung volumes. The daily GTV centroid position in the superior-inferior direction was strongly correlated with those of the ipsilateral and contralateral lung for 6 of 9 patients studied (r^2 = 0.51-0.98). The daily GTV centroid position was significantly associated with the contra-lateral lung volume for all patients (r^2 = 0.44, p < 0.05), but not with ipsi-lateral lung volume (r^2 = 0.02). A multivariate linear regression was computed with GTV daily centroid position as the dependent variable and daily contralateral lung volume and daily GTV volume as the independent variables over all patients. Both independent variables were significantly associated ($p < 0.05$) with the GTV daily position (r^2 = 0.76).

Tidal Volume Changes

Over all patients' 50 breathing traces (3 traces were not recorded due to operator error), the systematic baseline variation in tidal volume with respect to zero was marginal, although the variability in this measure was substantial ($M_\mu \pm \Sigma_\mu = 0.02 \pm 0.16$ L). On average, the pattern variation over all patients was not remarkable ($M_\sigma \pm \Sigma_\mu = 0.02 \pm 0.06$ L). Increasing mean daily tidal volume as significantly associated with an increase in the ipsilateral lung volume (r^2 = 0.58, $p < 0.05$). A two-tailed t-test between mean tidal volume of the first and last breathing sessions revealed no significant difference caused by timepoint in the treatment course (p = 0.84). For 4 patients, mean tidal volume was found to be strongly associated with tumor reduction (r^2 = 0.7-0.9). One patient showed a higher mean daily tidal volume (0.14 ± 0.06 L) than the population average, with mean daily tidal volume increasing with each fraction (r^2 = 0.7) (Figure 4).

DISCUSSION

This study was designed to evaluate the inter- and intra-fraction variability of tumor and lung position and volume during a hybrid breath-hold gating technique throughout radiation therapy. Inter-breath reproducibility in GTV and lung volumes better than 2.0 mm on average was observed with our hybrid breath-hold gating approach. Inter-fraction variability of GTV position in relation to bony anatomy under breath-hold was substantial. Inter-fraction variability of the lung was a substantial contributor. Increasing daily tidal volume was associated with increasing ipsilateral lung volume at breath-hold, although the relative breath-hold threshold was held at the same lung volume throughout treatment. Possibly, changes in tidal volume also influence functional residual capacity, that most likely explain the interfraction variation in lung volume. The ABC device uses functional residual capacity as a baseline for setting the breath hold volume, hence variations in functional residual capacity will manifest as changes in the breath hold lung volume. Notably, the daily tumor positions were strongly correlated with both the ipsilateral and contralateral lung positions in 67% of the patients studied. For the population, the tumor position was only significantly associated with contralateral lung volume. Pathological change, including atelectasis and pleural effusion, was observed in three patients in the ipsilateral lung. One patient also exhibited fluid accumulation in both lungs over the treatment course due to pneumonia. Changes in lung volume due to pathological changes may or may not impact the GTV position, depending on the severity and location. However, changes in healthy contralateral lung volume are most likely due to differences in the breath-hold lung volume, which directly impacted the GTV position. Online target-based image guidance is the suggested method to mitigate this effect. Because both the

systematic inter-fraction GTV positional variability and daily GTV position were strongly associated with tumor reduction, a substantial portion of inter-fraction variation can likely be attributed to tumor response. The variability of the tumor borders observed here demonstrates that lung tumor volume regression is non-uniform about the original centroid. The geometry of the change in gross tumor volume is likely a function of a large number of parameters including the dose distribution, mass effect of the tumor on surrounding normal anatomy, and presence of necrotic tissue, among others. Caution should be taken when performing target-based localization in the presence of substantial non-uniform tumor volume regression, as it is unknown how the effect will impact the quality of the planned dose distribution as well as coverage of residual microscopic extension of disease.

Cheung *et al.* evaluated the reproducibility of lung tumor position with ABC and found the average GTV displacement was better than 1.1 mm over the first five days of treatment (13). Kashani *et al.* investigated the intra- and inter-fraction variability of lung tumor position under breath-hold before the start of treatment, at 40%, and 80% of the prescribed total dose (12). Results of the current study were consistent, although with the added value of longitudinal data throughout the treatment course.

Systematic baseline variation in tidal volume was not significant for the population, although specific subjects had variations up to ~10% of the average volume threshold implemented for breath-hold (0.84 L). One patient had a higher mean daily tidal volume as his treatment progressed. Further investigation revealed increased fluid accumulation in the affected lung (pleural effusion) throughout treatment, presumably instigating breathing pattern changes (Figure 4). While the ipsilateral lung could not be evaluated due to the presence of fluid (and hence, lung volume changes not necessarily attributable to breath-hold), a strong correlation ($r^2 = 0.93$) was observed between the patient's daily GTV centroid position and the contralateral lung. This suggests the need to exercise caution in the implementation of ABC when pathological changes, such as pleural effusion or atelectasis, occur as these may impact target localization or fidelity of the planned dose distribution. Image-guided adaptive radiotherapy techniques will be required to address tumor volume change as well as these other pathological changes during therapy.

Similar to the current study, large systematic errors were observed in several patients by both Panakis *et al.*(14) and Sarrut *et al.* (9) The authors independently postulated that these large errors were due to tumor response or pathological changes during treatment. Errors were calculated across only two scans during treatment (in addition to a reference scan), so trends could not be assessed. In the current study, we were able to determine the trending of GTV position error due to the higher frequency of imaging. The drift in tumor position over the treatment course observed here limits the utility of the concept of systematic and random error for margin calculation (which relies on the assumption of a random, stationary process). Furthermore, the large variation in GTV position error among patients suggests that a single population margin is not the optimal solution for this cohort of patients. Patient-specific techniques such as image-guided and/or image-guided adaptive radiotherapy are warranted to reduce the margin requirement and to compensate for the non-stationary GTV position during treatment. However, the efficient implementation of online image-guidance for breath-hold of lung cancer patients is still under development (22).

Patient compliance has been suggested as a limitation in active breath-hold radiotherapy of the lung, however statistical comparisons in both GTV positional variability and mean tidal volume between first and last imaging sessions revealed insignificant differences. These results support the implementation of a hybrid breath-hold gating technique throughout lung cancer treatment, particularly late in the treatment course, where patient performance and breathing stability may be affected.

The current study has several limitations that may impact the results. Five of the nine patients had upper lobe tumors, which may result in lower mobility and overall lower variability, at least for free-breathing patients (7). In breath hold patients, it is not clear that the variability would trend similarly as for free-breathing patients, due to the different mechanics of breath hold. Furthermore, it is not known whether tumor regression is associated with tumor location, and tumor regression was a substantial contributor to the variability in this study. Subgroup analysis in a larger cohort is underway to evaluate tumor location effects. Delineation was performed to achieve the highest precision possible through assistance by deformable image registration and careful review by a physician. However, delineation error most likely remains a contributor to the total error burden in our study. Our findings for the spinal cord (<1 mm inter-breath hold variability) demonstrate that minimal systematic error was introduced through in the delineation and structure propagation process, thus adding confidence in our approach. However, the error level for other structures was not be quantified.

CONCLUSION

Intrafraction breath-hold reproducibility better than 2 mm was observed for the hybrid active breath hold gating technique, although inter-fraction variability of GTV position was substantial, mainly due to tumor regression and changes in breath-hold lung volume over treatment. These results support the implementation of a hybrid active breath-hold gating technique for lung cancer treatment, particularly late in the treatment course, where patient performance and breathing stability may be affected. However, the necessity of image-guided adaptive radiotherapy techniques must be emphasized to reduce target margins and reduce the impact of tumor regression on tumor stability under breath-hold.

Acknowledgments

The authors would like to thank Tiezhi Zhang, PhD for assistance with deformable registration. The authors would also like to thank Ana Paula Galerani, M.D. and Samuel McGrath, M.D. for contouring assistance and consultation. Supported in part by National Cancer Institute Grant R01CA116249.

REFERENCES

1. Britton KR, Starkschall G, Tucker SL, et al. Assessment of gross tumor volume regression and motion changes during radiotherapy for non-small-cell lung cancer as measured by four-dimensional computed tomography. Int J Radiat Oncol Biol Phys 2007;68:1036–1046. [PubMed: 17379442]
2. Hugo G, Vargas C, Liang J, et al. Changes in the respiratory pattern during radiotherapy for cancer in the lung. Radiother Oncol 2006;78:326–331. [PubMed: 16564592]
3. Juhler Nottrup T, Korreman SS, Pedersen AN, et al. Intra- and interfraction breathing variations during curative radiotherapy for lung cancer. Radiother Oncol 2007;84:40–48. [PubMed: 17588697]
4. Liu HH, Balter P, Tutt T, et al. Assessing respiration-induced tumor motion and internal target volume using four-dimensional computed tomography for radiotherapy of lung cancer. Int J Radiat Oncol Biol Phys 2007;68:531–540. [PubMed: 17398035]
5. Mageras GS, Pevsner A, Yorke ED, et al. Measurement of lung tumor motion using respiration-correlated CT. Int J Radiat Oncol Biol Phys 2004;60:933–941. [PubMed: 15465212]
6. Seppenwoolde Y, Shirato H, Kitamura K, et al. Precise and real-time measurement of 3D tumor motion in lung due to breathing and heartbeat, measured during radiotherapy. Int J Radiat Oncol Biol Phys 2002;53:822–834. [PubMed: 12095547]
7. Sonke J-J, Lebesque J, van Herk M. Variability of Four-Dimensional Computed Tomography Patient Models. Int J Radiat Oncol Biol Phys 2008;70:590–598. [PubMed: 18037579]
8. Keall PJ, Mageras GS, Balter JM, et al. The management of respiratory motion in radiation oncology report of AAPM Task Group 76. Med Phys 2006;33:3874–3900. [PubMed: 17089851]

9. Sarrut D, Boldea V, Ayadi M, et al. Nonrigid registration method to assess reproducibility of breath-holding with ABC in lung cancer. Int J Radiat Oncol Biol Phys 2005;61:594–607. [PubMed: 15667982]
10. Wong JW, Sharpe MB, Jaffray DA, et al. The use of active breathing control (ABC) to reduce margin for breathing motion. Int J Radiat Oncol Biol Phys 1999;44:911–919. [PubMed: 10386650]
11. Remouchamps VM, Letts N, Yan D, et al. Three-dimensional evaluation of intra- and interfraction immobilization of lung and chest wall using active breathing control: A reproducibility study with breast cancer patients. Int J Radiat Oncol Biol Phys 2003;57:968–978. [PubMed: 14575827]
12. Kashani R, Balter JM, Hayman JA, et al. Short-term and long-term reproducibility of lung tumor position using active breathing control (ABC). Int J Radiat Oncol Biol Phys 2006;65:1553–1559. [PubMed: 16863932]
13. Cheung PC, Sixel KE, Tirona R, et al. Reproducibility of lung tumor position and reduction of lung mass within the planning target volume using active breathing control (ABC). Int J Radiat Oncol Biol Phys 2003;57:1437–1442. [PubMed: 14630283]
14. Panakis N, McNair HA, Christian JA, et al. Defining the margins in the radical radiotherapy of non-small cell lung cancer (NSCLC) with active breathing control (ABC) and the effect on physical lung parameters. Radiother Oncol 2008;87:65–73. [PubMed: 18267345]
15. Hirsch A, Vander Els N, Straus DJ, et al. Effect of ABVD chemotherapy with and without mantle or mediastinal irradiation on pulmonary function and symptoms in early-stage Hodgkin's disease. J Clin Oncol 1996;14:1297–1305. [PubMed: 8648387]
16. Jaen J, Vazquez G, Alonso E, et al. Changes in pulmonary function after incidental lung irradiation for breast cancer: A prospective study. Int J Radiat Oncol Biol Phys 2006;65:1381–1388. [PubMed: 16757130]
17. Erridge SC, Seppenwoolde Y, Muller SH, et al. Portal imaging to assess set-up errors, tumor motion and tumor shrinkage during conformal radiotherapy of non-small cell lung cancer. Radiother Oncol 2003;66:75–85. [PubMed: 12559524]
18. Murphy MJ, Martin D, Whyte R, et al. The effectiveness of breath-holding to stabilize lung and pancreas tumors during radiosurgery. Int J Radiat Oncol Biol Phys 2002;53:475–482. [PubMed: 12023152]
19. Zhang T, Chi Y, Meldolesi E, et al. Automatic delineation of on-line head-and-neck computed tomography images: toward on-line adaptive radiotherapy. Int J Radiat Oncol Biol Phys 2007;68:522–530. [PubMed: 17418960]
20. Lotz HT, Pos FJ, Hulshof MC, et al. Tumor motion and deformation during external radiotherapy of bladder cancer. Int J Radiat Oncol Biol Phys 2006;64:1551–1558. [PubMed: 16580504]
21. van Herk M, Remeijer P, Rasch C, et al. The probability of correct target dosage: dose-population histograms for deriving treatment margins in radiotherapy. Int J Radiat Oncol Biol Phys 2000;47:1121–1135. [PubMed: 10863086]
22. Thompson BP, Hugo GD. Quality and accuracy of cone beam computed tomography gated by active breathing control. Med Phys 2008;35:5595–5608. [PubMed: 19175117]

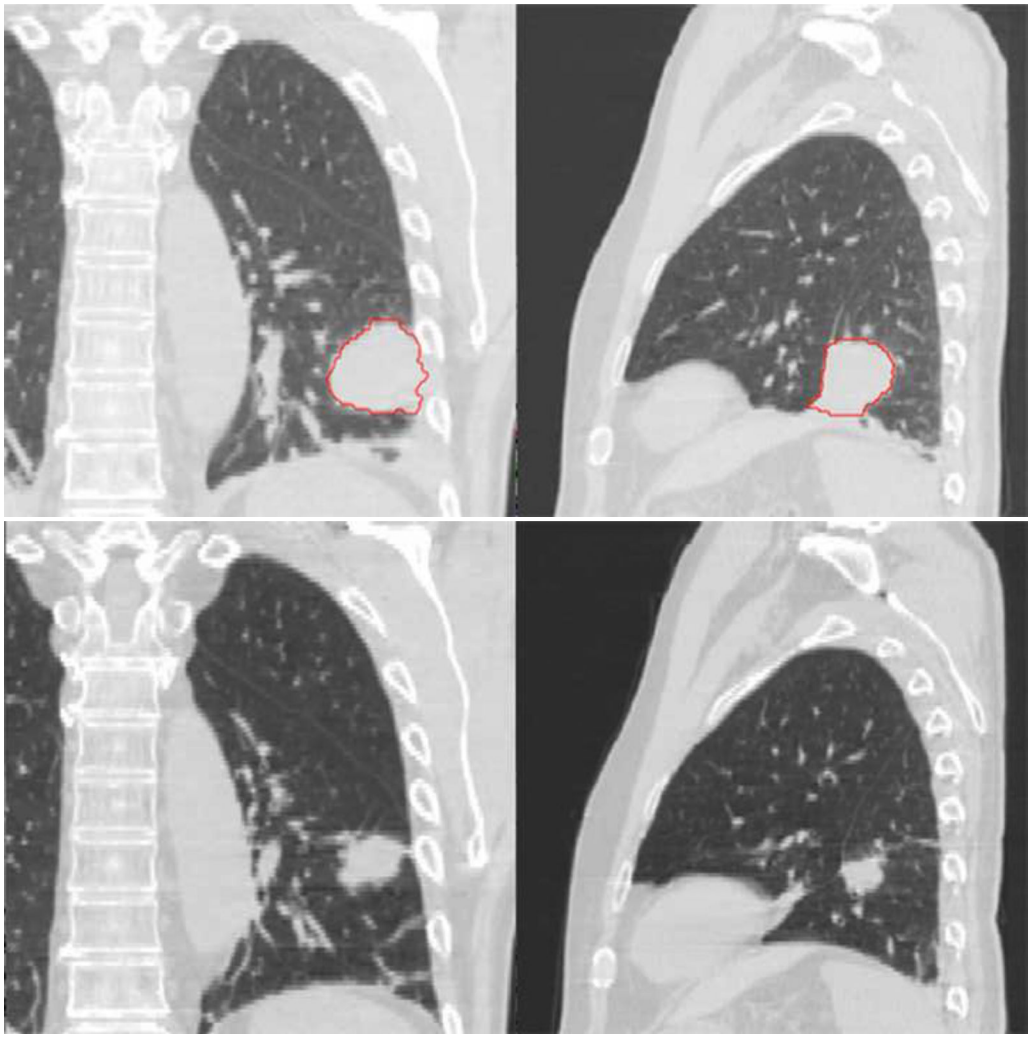

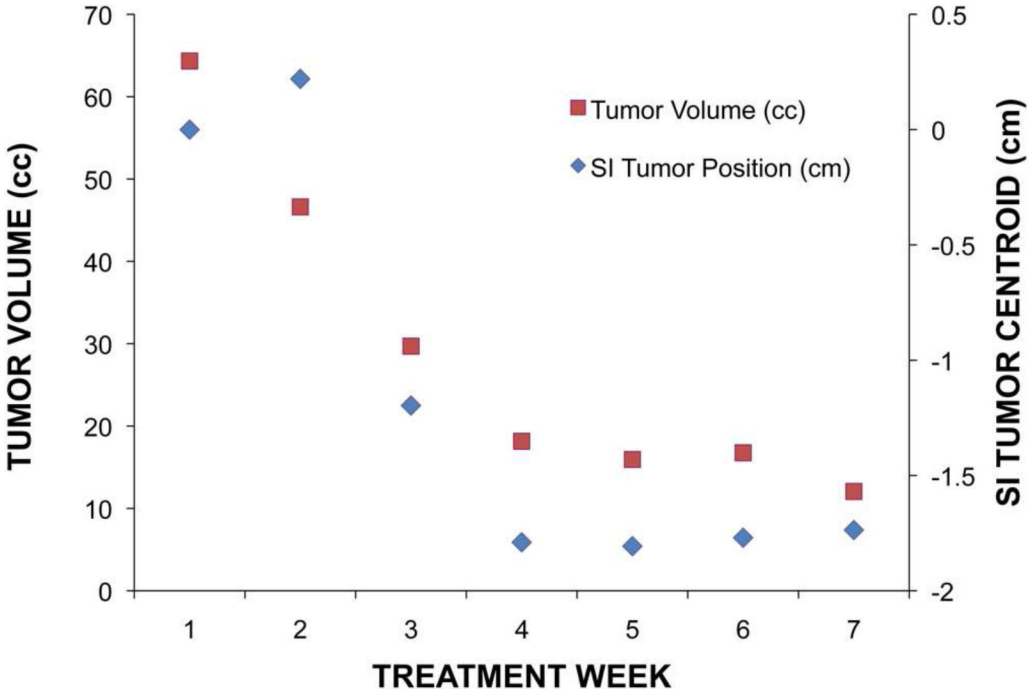

Figure 1.

First (a) and last (b) week breath-hold CT images for Patient 4. Substantial tumor volume regression is evident. GTV from the first week is shown in red. (c) Tumor centroid position relative to bone compared with the tumor volume. As the tumor volume changed, the position of the tumor centroid trended superiorly.

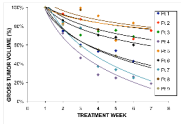

Figure 2.
Gross tumor volume, expressed as a percentage of the first week of treatment tumor volume, observed over the treatment course (n = 9). The individual logarithmic fits shown provided the best fit for the data on average.

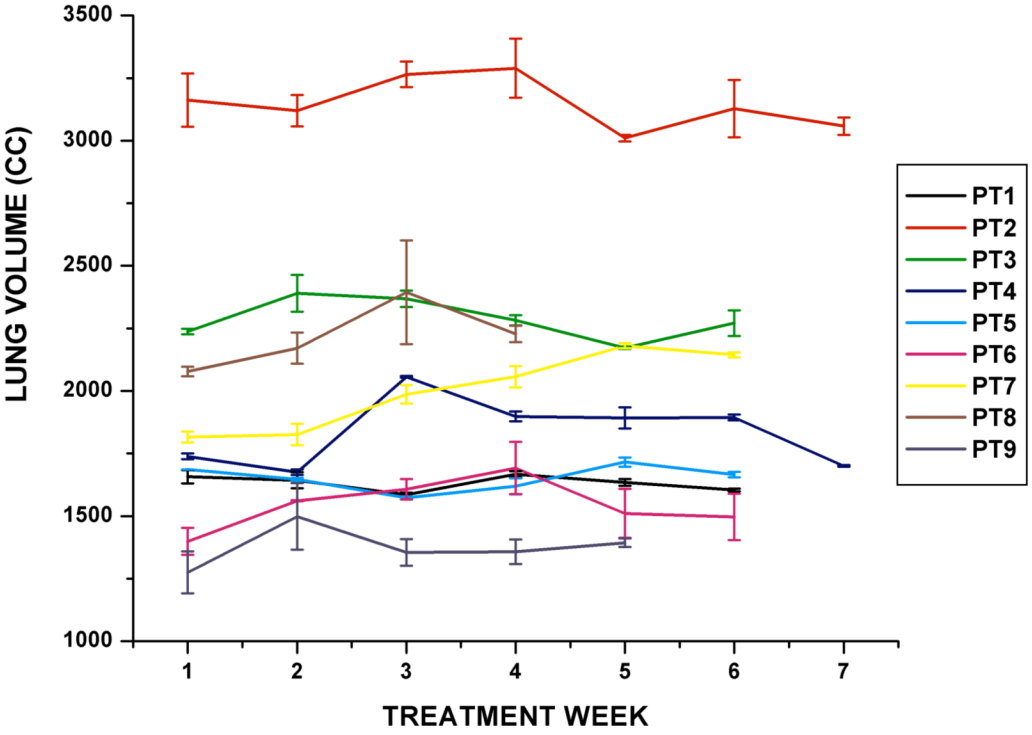

Figure 3.
Stability of the left lung volume under breath-hold observed over the treatment course for 9 patients. Each data point indicates the daily lung volume (mean ± standard deviation).

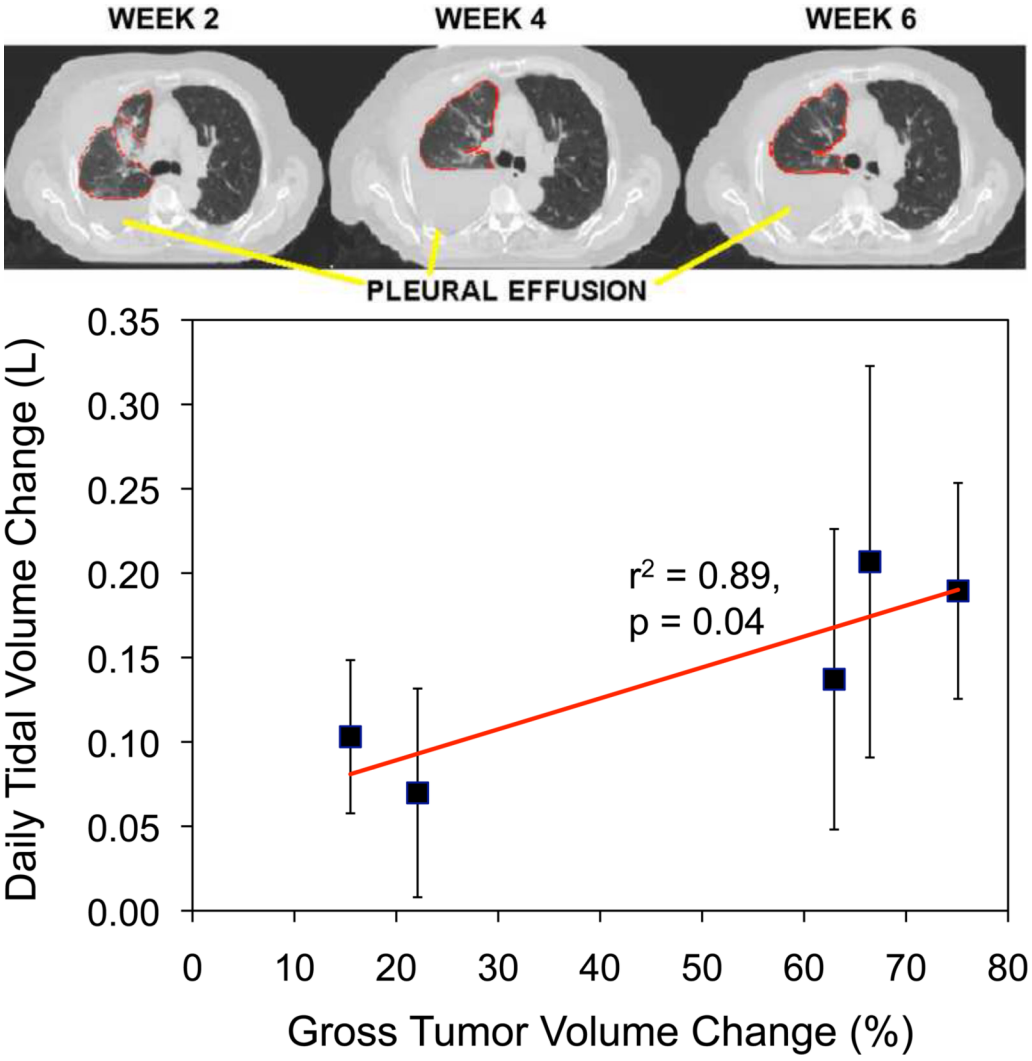

Figure 4.

(a) Patient 7 had increased fluid in his affected lung (pleural effusion), which impacted inter-fraction stability of the tumor throughout treatment. This patient also had the largest systematic error in the study population, emphasizing the importance of image-guided adaptive radiotherapy. (b) For Patient 7, change in daily tidal volume with respect to change in gross tumor volume size over treatment.

Table 1

Patient demographics for normal-inspiration breath-hold imaging study.

Patient	GTV Location	TNM Stage	CT Scans	Histology
1	LUL	T2N2M0	18	Sq. CC
2	RLL	T3N0M0	21	Sq. CC
3	Bilateral	T4N2MX	18	Sq. CC
4	LLL	T2N1M0	21	Adeno
5	RUL	T1N3M0	18	Large CC
6	RLL	T2N2M0	18	NOS
7	RUL	T3N2M1	18	Adeno
8	RUL	T2N1M0	12	Sq. CC
9	RUL	T2N2M0	15	Sq. CC

Abbreviations: LUL, left upper lobe; RLL, right lower lobe; LLL, left lower lobe; RUL, right upper lobe; Sq. CC, squamous cell carcinoma; Adeno, adenocarcinoma; NOS, not otherwise specified; GTV, gross tumor volume.

Table 2

Inter-breath hold variability (mm) of the GTV, left and right lung centroids over all imaging sessions. Mean, standard deviation, and range of the quantities are reported for the study population. L-R, A-P, and S-I represent left to right, anterior to posterior, and superior to inferior, respectively.

	Inter-breath hold variability (mm) Mean +/− standard deviation (range)		
Structure	**L-R**	**A-P**	**S-I**
GTV	0.6 +/− 0.3 (0.1-1.0)	1.0 +/− 0.5 (0.2-1.6)	1.4 +/− 1.0 (0.3-1.8)
Left Lung	0.5 +/− 0.4 (0.1-1.5)	1.0 +/− 0.7 (0.2-2.0)	2.1 +/− 1.3 (0.5-4.1)
Right Lung	0.6 +/− 0.5 (0.2-1.6)	1.0 +/− 0.6 (0.4-2.0)	1.8 +/− 1.2 (0.7-3.8)

Table 3

Population results for systematic and random errors in tumor, left lung, right lung, and spinal cord position relative to the first ABC helical CT scan (n = 9, except for right lung where one patient was excluded due to pleural effusion). All data reported in mm.

	GTV			Left Lung			Right Lung			Spinal Cord		
	L-R	**A-P**	**S-I**	**L-R**	**A-P**	**S-I**	**L-R**	**A-P**	**S-I**	**L-R**	**A-P**	**S-I**
Systematic Error (Σ)	3.6	3.9	6.7	1.4	1.3	3.4	1.0	0.7	3.3	0.8	0.7	2.0
Random Error (σ)	3.1	3.1	3.9	1.5	1.7	2.6	1.5	1.2	2.6	0.8	0.5	1.6

Abbreviations: L-R, A-P, and S-I represent left to right, anterior to posterior, and superior to inferior, respectively.

Int J Radiat Oncol Biol Phys. Author manuscript; available in PMC 2011 July 1.

Table 4

Interfraction variation in gross tumor volume border position relative to the first ABC helical CT scan (n = 9), for the study population, as determined by bounding-box analysis . All data reported in mm.

	Left	Right	Ant	Post	Sup	Inf
Group Mean (M)	2.8	−0.7	0.8	4.5	0.7	−0.1
Systematic Error (Σ)	3.7	3.5	2.2	6.6	6.3	6.1
Random Error (σ)	3.3	2.5	2.8	3.8	4.6	6.9

Abbreviations: Ant, Post, Sup, and Inf represent anterior, posterior, superior, and inferior tumor borders, respectively.

Table 5

Patient-specific random inter-fraction error of gross tumor volume bounding box relative to the first ABC helical CT scan (n = 9), oriented along the axis of maximum variance. 'Minimum box corner' is the 3D position of the right, posterior, superior box corner surrounding the GTV; 'Maximum box corner' is the 3D position of the left, anterior, inferior box corner surrounding the GTV; 'Centroid' is the 3D position of the GTV centroid. All data reported in mm.

Patient	Minimum Box Corner	Centroid	Maximum Box Corner	RMS
1	2.8	3.5	2.5	3.6
2	4.4	2.5	3.2	4.3
3	7.9	4.9	2.3	6.8
4	7.6	8.8	17.4	14.8
5	1.1	1.0	0.9	1.2
6	3.8	5.6	14.7	11.4
7	14.7	9.2	5.2	12.8
8	2.3	2.2	1.8	2.6
9	2.3	2.0	2.5	2.8

Abbreviations: RMS = root mean square of minimum, centroid, and maximum positions.